Since January 2020 Elsevier has created a COVID-19 resource centre with free information in English and Mandarin on the novel coronavirus COVID-19. The COVID-19 resource centre is hosted on Elsevier Connect, the company's public news and information website.

Polyhedron 115 (2016) 164–173

Contents lists available at ScienceDirect

Polyhedron

journal homepage: www.elsevier.com/locate/poly

Electrophilic and nucleophilic pathways in ligand oxide mediated reactions of phenylsulfinylacetic acids with oxo(salen)chromium(V) complexes

P. Subramaniam [a,*], S. Sugirtha Devi [b], S. Anbarasan [a]

[a] Research Department of Chemistry, Aditanar College of Arts and Science, Tiruchendur 628 216, Tamil Nadu, India
[b] Department of Chemistry, Kamaraj College, Thoothukudi 628 003, Tamil Nadu, India

ARTICLE INFO

Article history:
Received 31 January 2016
Accepted 5 May 2016
Available online 13 May 2016

Keywords:
Oxo(salen)chromium(V)
Phenylsulfinylacetic acid
Single electron-transfer
Non-linear Hammett plot
Michaelis–Menten kinetics

ABSTRACT

The mechanism of oxidative decarboxylation of phenylsulfinylacetic acids (PSAA) by oxo(salen)$Cr(V)^+$ ion in the presence of ligand oxides has been studied spectrophotometrically in acetonitrile medium. Addition of ligand oxides (LO) causes a red shift in the λ_{max} values of oxo(salen) complexes and an increase in absorbance with the concentration of LO along with a clear isobestic point. The reaction shows first-order dependence on oxo(salen)-chromium$(V)^+$ ion and fractional-order dependence on PSAA and ligand oxide. Michaelis–Menten kinetics without kinetic saturation was observed for the reaction. The order of reactivity among the ligand oxides is picoline N-oxide > pyridine N-oxide > triphenylphosphine oxide. The low catalytic activity of TPPO was rationalized. Both electron-withdrawing and electron-donating substituents in the phenyl ring of PSAA facilitate the reaction rate. The Hammett plots are non-linear upward type with negative ρ value for electron-donating substituents, (ρ^- = −0.740 to −4.10) and positive ρ value for electron-withdrawing substituents (ρ^+ = +0.057 to +0.886). Non-linear Hammett plot is explained by two possible mechanistic scenarios, electrophilic and nucleophilic attack of oxo(salen)chromium$(V)^+$-LO adduct on PSAA as the substituent in PSAA is changed from electron-donating to electron-withdrawing. The linearity in the log$k$ vs. E_{ox} plot confirms single-electron transfer (SET) mechanism for PSAAs with electron-donating substituents.

1. Introduction

Oxygen transfer is so common and important in biological systems as well as in chemical synthesis. Because of the easy preparation, reasonable stabilities, biological activities etc., salen ligand [salen = 1,6-bis(2-hydroxyphenyl)-2,5-diazahexa-1,5-diene], its derivatives and their associated metal complexes are widely used as potential catalysts in oxo transfer reactions [1–5] and many other processes [6–11]. They also mimic enzymatic reactions [12,13]. Further, the applications of N-oxide derivatives have received considerable attention due to their usefulness as synthetic intermediates and biological importance. Pyridine N-oxide derivatives represent a new class of anti-HIV compounds and oxide part of the pyridine moiety proved to be indispensable for anti-coronavirus activity. The potential and virus specificity of the pyridine N-oxides were shown to vary depending on the nature and location of the substituents in the molecule [14]. Heterocyclic N-oxides are used as protecting groups, auxiliary agents, oxidants, ligands in metal complexes and catalysts [15] besides bio-reductive drugs [16]. Hence the study of the role and action of N-oxides on the activity of metallo-enzymes are of biological importance.

Over a past few decades, a variety of effects have been reported with different additives for various reactions [17–22] and different explanations have been given for these effects. Although, a large number of reports on the reactivity of oxo metal complexes with nitrogen bases as additives [23–27] have appeared in the literature only little interest has been paid by using ligand oxides as additives in these reactions. Even in majority of cases where ligand oxides are used as additive, no effect is observed in epoxidation [28] and sulfoxidation reactions [29–33]. Further, there was no detailed

Abbreviations: PSAA, phenylsulfinylacetic acid; salen, N,N′-bis(salicylidene)-ethylenediaminato; LO, ligand oxide; TPPO, triphenylphosphine oxide; PyO, pyridine N-oxide; PicNO, picoline N-oxide; OD, optical density; SET, single electron-transfer.

* Corresponding author. Tel.: +91 9443500381.
E-mail addresses: subramaniam.perumal@gmail.com (P. Subramaniam), sugirthadevi.s@gmail.com (S. Sugirtha Devi), sanbarasan62@gmail.com (S. Anbarasan).

http://dx.doi.org/10.1016/j.poly.2016.05.012
0277-5387/

mechanistic study on the oxidation of phenylsulfinylacetic acid (PSAA) except our recent publications on the proximal effects of nitrogen bases with oxo(salen)Cr(V)$^+$ ion [34] and Cr(VI) oxidation of PSAA [35] mediated by cetyltrimethylammonium bromide [36], oxalic acid [37] and picolinic acid [38], though PSAA is a versatile synthetic agent used for the synthesis of antibiotics [39] and various organic compounds [40–44]. Out of our much interest on the oxidation studies of sulfur compounds especially with PSAA in the presence of additives and a significant effect observed with ligand oxides, detailed kinetic investigation on the reactions between PSAAs and oxo(salen)chromium(V) complexes in the presence of triphenylphosphine oxide (TPPO), pyridine N-oxide (PyO) and picoline N-oxide (PicNO) has been carried out. The following scheme (Scheme 1) summarises the work described in this paper.

2. Experimental

2.1. Preparation of (salen)chromium(III) chloride

(Salen)chromium(III) chloride was synthesized by the established procedure [45]. Chromium(III) chloride hexahydrate (0.01 M, 2.5 g) dissolved in minimum amount of distilled water was reduced to chromium(II) chloride by Zn/Hg under nitrogen atmosphere. The blue color solution of chromium(II) chloride formed was added in drops to a suspension of salen ligand (0.008 M, 2.15 g) in 30 ml of acetone under nitrogen atmosphere. After exposing the resulting dark brown solution in air, it was heated to reflux for 1 h. The wet residue obtained after the removal of solvent was stirred with water for 2 h. The (salen)chromium(III) chloride formed was filtered, washed with dichloromethane and saturated NH_4Cl followed by aqueous sodium chloride. By adopting a similar procedure (5,5′-dichlorosalen)Cr(III) chloride and (5,5′-dimethylsalen)Cr(III) chloride were prepared. The (salen)chromium(III) chloride complexes were recrystallized from methanol–water mixture. The salen, 5,5′-dichloro and 5,5′-dimethyl substituted salen ligands were prepared by refluxing the corresponding salicylaldehyde and ethylenediamine in ethanol.

2.2. Preparation of (salen)chromium(III) hexafluorophosphate

In order to get better solubility of Cr(III) complexes, (salen)chromium(III) chloride was converted into (salen)chromium(III) hexafluorophosphate by crystallizing from an equimolar mixture of (salen)chromium(III) chloride in methanol–water and ammonium hexafluorophosphate in minimum amount of water [46]. The dried samples were stored in the refrigerator at 0 °C. As the concentrations of oxo(salen)chromium(V)$^+$ PF_6^- complexes were determined on the basis of concentration of (salen)chromium(III)$^+$ PF_6^-, their purity were confirmed by elemental micro analyses and characterized by UV–vis. spectroscopy (Supporting information Fig. S1). The same λ_{max} values were reported for these complexes by Premsingh et al. [47].

(Salen)Cr(III)$^+$ PF_6^-, *Anal.* Calc. for $C_{16}H_{14}O_2N_2CrPF_6$: C, 41.48; H, 3.05; N, 6.05. Found: C, 41.35; H, 3.12; N, 5.95%. UV–vis (λ_{max}): 228, 285, 317, 360, 415 nm.

5,5′-(Me_2salen)Cr(III)$^+$ PF_6^-, *Anal.* Calc. for $C_{18}H_{18}O_2N_2CrPF_6$: C, 44.01; H, 3.69; N, 5.70. Found: C, 44.21; H, 3.75; N, 5.60%. UV–vis (λ_{max}): 227, 286, 328, 429 nm.

5,5′-(Cl_2salen)Cr(III)$^+$ PF_6^-, *Anal.* Calc. for $C_{16}H_{12}O_2N_2Cl_2CrPF_6$: C, 36.11; H, 2.27; N, 5.27. Found: C, 36.25; H, 2.21; N, 5.23%. UV–vis (λ_{max}): 228, 288, 325, 427 nm.

2.3. Synthesis of oxo(salen)chromium(V)$^+$ PF_6^- complexes

A slight excess of iodosobenzene (0.0051 M, 0.06 g) was added to (salen)chromium(III) hexafluorophosphate (0.005 M, 0.116 g) dissolved in 50 ml of acetonitrile. The solution was stirred for 30 min and then filtered to remove the unreacted iodosobenzene. The color of the solution turned from red orange to dark green brown. The dark green solution of oxo(salen)chromium(V)$^+$ ion was used for the kinetic study after subsequent dilution. Following the above procedure, other substituted oxo(salen)Cr(V)$^+$ PF_6^- complexes (**Ib** & **Ic**) were prepared and characterised by their UV–vis absorption spectra which are identical with the previous report [47].

2.4. Preparation of phenylsulfinylacetic acids

Phenylmercaptoacetic acids and its substituted acids were prepared using established procedure [48,49] by refluxing the corresponding thiophenols with chloroacetic acid in alkaline medium for 5–6 h. Phenylmercaptoacetic acids were converted into corresponding phenylsulfinylacetic acids by controlled oxidation with equimolar hydrogen peroxide [50] and were recrystallised with suitable solvent mixture. The purity of PSAAs was checked by elemental micro analyses, melting point and LC–MS analysis. The LC–MS spectrograms are recorded in APCI (-) mode and are shown in the Supporting information Fig. S2. The melting points determined for different PSAAs are found to agree with those reported in the literature [48,50].

PSAA[a]: Mp.: 115–117 °C. Mass Spec.: Calc. 183 amu. Found: 183.1 amu. *Anal.* Calc.: C, 52.17; H, 4.35; Found: C, 52.08; H, 4.30%.

p-OMe PSAA[a]: Mp: 104 °C. Mass Spec.: Calc.: 214 amu. Found: 213.1 amu. *Anal.* Calc.: C, 50.47; H, 4.67; Found: C, 50.58; H, 4.70%.

p-OEt PSAA[a] Mp: 124–125 °C. Mass Spec.: Calc.: 228 amu. Found: 226.9 amu. *Anal.* Calc.: C, 52.63; H, 5.26; Found: C, 52.58; H, 5.30%.

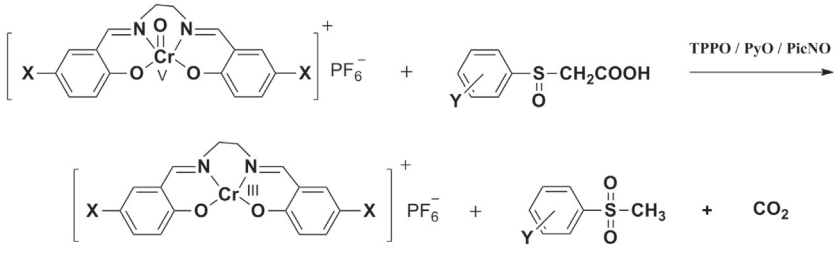

Ia : X = H; **Ib** : X = CH_3; **Ic** : X = Cl

PSAA : Y = *p*-OMe, *p*-OEt, *p*-Me, *m*-Me, H, *p*-F, *p*-Cl, *m*-F, *m*-Cl, *p*-NO_2

Scheme 1. Oxidative decarboxylation of PSAA by oxo(salen)Cr(V)$^+$ ion.

p-Me PSAA[b] Mp: 104 °C. Mass Spec.: Calc.: 198 amu. Found: 197.2 amu. *Anal.* Calc.: C, 54.55; H, 5.05; Found: C, 54.60; H, 5.09%.

m-Me PSAA[b] Mp: 88 °C. Mass Spec.: Calc.: 198 amu. Found: 197.0 amu. *Anal.* Calc.: C, 54.55; H, 5.05; Found: C, 54.48; H, 5.01%.

p-F PSAA[a] Mp: 122 °C. Mass Spec.: Calc.: 202 amu. Found: 200.9 amu. *Anal.* Calc.: C, 47.52; H, 3.47; Found: C, 47.48; H, 3.42%.

p-Cl PSAA[a] Mp: 127–128 °C. Mass Spec.: Calc.: 218.5 amu. Found: 217.3 amu. *Anal.* Calc.: C, 43.94; H, 3.20; Found: C, 44.01; H, 3.22%.

m-F PSAA[a] Mp: 103 °C. Mass Spec.: Calc.: 202 amu. Found: 201.1 amu. *Anal.* Calc.: C, 47.52; H, 3.4; Found: C, 47.55; H, 3.46%.

m-Cl PSAA[a] Mp: 109 °C. Mass Spec.: Calc.: 218.5 amu. Found: 217.7 amu. *Anal.* Calc.: C, 43.94; H, 3.20; Found: C, 43.89; H, 3.16%.

p-NO_2 PSAA[c] Mp: 167 °C. *Anal.* Calc.: C, 41.92; H, 3.06; Found: C, 41.97; H, 3.10%.

Recrystallizing solvent: [a]ethyl acetate-benzene (1:1); [b]chloroform-petroleum ether (1:1); [c]aqueous acetone (1:1).

Salicylaldehyde and various substituted salicylaldehydes (Alfa Aeser), $CrCl_3.6H_2O$ (Sigma Aldrich), pyridine N-oxide (SIGMA–ALDRICH), triphenylphosphine oxide (Alfa Aesar), picoline N-oxide (SIGMA–ALDRICH), thiophenol (S D fine) and substituted thiophenols (SIGMA ALDRICH) were purchased and used as such. H_2O_2 (GR, Merck) and acetonitrile (HPLC grade, Merck) were used as received.

2.5. Stoichiometry and product analysis

The stoichiometry of the reaction between O=Cr^V(salen) complex and PSAA was found to be 1:1 from the study of mixing different ratios of concentration of oxo(salen) and PSAA. The reaction mixtures containing equivalent moles of PSAA (0.6 mM) and oxo (salen)chromium(V)$^+$ ion (0.6 mM) in acetonitrile in the presence of ligand oxides (kinetic run concentration) were kept aside for two days at room temperature for completion of the reaction which is shown from the reappearance of brown color of (salen) chromium(III) complex from the deep green color. After the completion of the reaction, the solvent was removed in vaccum; the residue was extracted with diethyl ether and dried over anhydrous sodium sulfate. The organic product formed during the reaction was characterised as methyl phenyl sulfone by LC–MS (Supporting information Fig. S3), GC–MS (Supporting information Fig. S4) and IR (Supporting information Fig.S5) spectral methods.

2.6. Cyclic voltammetry

Cyclic voltammetric (CV) studies were performed using CH instrument model CHI 650C in acetonitrile medium containing 0.1 M tetrabutyl ammonium perchlorate as the supporting electrolyte. The voltammetry utilizes a three electrode configuration. The glassy carbon electrode is the working electrode at which the electrolysis takes place. The current required to sustain electrolysis is provided by the counter electrode namely platinum electrode that is directly placed into the solution. The reference electrode is Ag/AgCl electrode. Cyclic voltammograms are obtained by measuring the current at the working electrode during the potential change. Cyclic voltammograms were recorded at the sweep rate of 0.05 V/s in the scan range of +1.4 V to −0.4 V for oxo(salen) chromium(V)$^+$ ions and at the sweep rate of 0.1 V/s in the scan range of −1 V to +1.4 V for PSAAs.

3. Results and discussion

The complexes **Ia**, **Ib** and **Ic** have an absorption maximum (λ_{max}) at 560 nm, 557 nm and 584 nm respectively in 100% acetonitrile medium. Additions of ligand oxide/PSAA to the complex shift the λ_{max} appreciably to higher wavelength along with an immediate color change to emerald green.

The shift in the λ_{max} is in the range of 13 nm–78 nm and the observed λ_{max} values in the presence and absence of additives are recorded in Table 1. The shift in the λ_{max} value on adding ligand oxide/PSAA to the oxo(salen) complex indicates binding of LO/PSAA with oxo(salen)chromium(V)$^+$ to form adduct.

3.1. Determination of binding constants between complex and ligand oxide

The binding constants for the formation of adduct between ligand oxides viz. TPPO, PyO, PicNO and oxo(salen)chromium(V)$^+$ ions (**Ia–Ic)** were determined by absorption spectroscopy. Absorption spectral titration experiments were carried out by keeping the concentration of oxo(salen)chromium(V)$^+$ complex constant (5×10^{-4} M) and varying the ligand oxide concentrations by maintaining the total volume of the reaction mixture as constant. Increase in concentrations of ligand oxide to the oxo(salen) complex showed both hyperchromicity and red shift in the absorption maxima for all the three complexes. The representative absorption spectral changes observed during the titration processes are shown in Fig. 1. The spectral titration curves of the oxo(salen) complexes with ligand oxides show the existence of isobestic point. This confirms the formation of 1:1 adduct between ligand oxide and the oxo(salen) complex in a reversible process.

The absorbance reading (OD) of complexes at different ligand oxide concentrations in the maximum absorption was recorded and the binding constant (K_f) for the adduct formation was evaluated using the modified Benesi–Hildebrand equation (Eq. (1)) and plot [51,52]. The calculated binding constant values are recorded in Table 2.

$$\frac{[\text{oxo(salen)}]\ [\text{LO}]}{\Delta(\text{OD})} = \frac{[\text{oxo(salen)}] + [\text{LO}]}{\Delta\varepsilon} + \frac{1}{K_f \Delta\varepsilon} \quad (1)$$

The binding constant value depends on the nature of the ligand oxide as well as the nature of the substituent in the salen ligand. Electron-donating methyl substituent in the 5 and 5′-positions of the salen complex shows low binding constant while the electron-withdrawing chloro substituent has high binding constant value compared with the unsubstituted salen complex. Among the three ligand oxides used in the study, TPPO has the least binding constant. The low binding constant values with TPPO is expected because of its bulky nature. Thus the observed trend of binding constant indicates the involvement of a substantial steric inhibition during adduct formation between ligand oxides and oxo(salen) complexes. The enormous shift along with increase in absorbance in the λ_{max} value of oxo(salen)chromium(V)$^+$ by the addition of ligand oxides and the observed large binding constant values support the strong binding of ligand oxides with the metal centre resulting in the formation of LO → Cr^Voxo(salen) adduct.

Table 1
λ_{max} values of oxo(salen)chromium(V)$^+$ PF_6^- complexes in the presence of PSAA and ligand oxides.

Complex	λ_{max} (nm) in the presence of additives							
	Without additive	PSAA	TPPO		PyO		PicNO	
		a	b	c	b	c	b	c
Ia	560	584	613	595	612	597	612	598
Ib	557	570	633	621	635	630	627	617
Ic	584	622	640	627	627	627	627	622

[a]oxo(salen) + PSAA.
[b]oxo(salen) + LO.
[c]oxo(salen) + PSAA + LO.

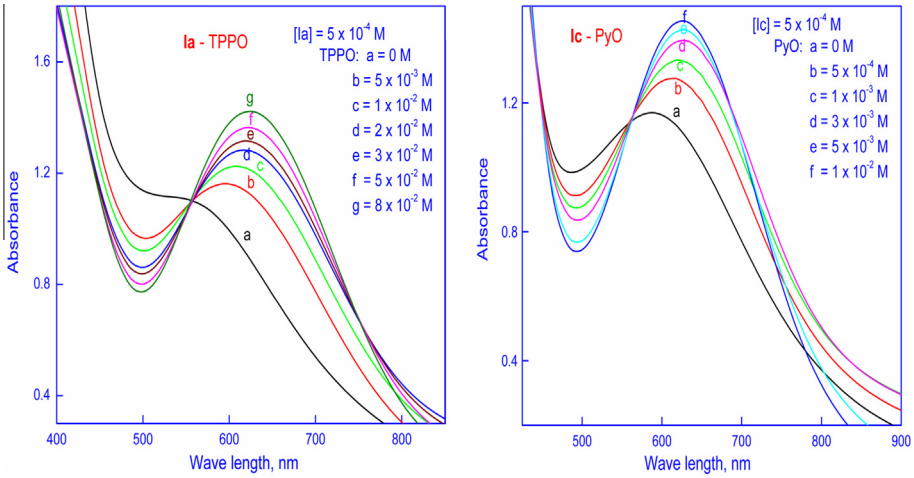

Fig. 1. Absorption changes of **Ia** and **Ic** during spectral titration with ligand oxides.

Table 2
Binding constant values of **Ia-Ic** with ligand oxides.

Complex	Binding constant (M^{-1})		
	TPPO	PyO	PicNO
Ia	49.0	1817	747
Ib	40.8	985	78.6
Ic	129	3160	1892

This was supported by the work of Kochi and co-workers [28,45] who have isolated the oxo(salen)chromium(V)$^{+}$-PyO adduct and reported their X-ray analysis data. Though they isolated the adduct of sterically hindered oxo(salen), dichlorotetramethyloxo(salen) with PyO, they were unable to isolate adduct with other LOs and salen complexes.

3.2. Kinetic study

The kinetic study for the oxidative decarboxylation of PSAAs with oxo(salen)Cr(V)$^{+}$ ions (**Ia**–**Ic**) in the presence of ligand oxides were carried out spectrophotometrically at 303 K under pseudo-first-order conditions in 100% acetonitrile medium using excess of PSAA over oxo(salen)Cr(V)$^{+}$ ion concentration in the ratio of at least 100:1. The concentration of oxo(salen)Cr(V)$^{+}$ ion was maintained at 5×10^{-4} M unless or otherwise specified and the concentration of substrate, PSAA was maintained in the range of 0.05 M to 0.4 M. The concentration of ligand oxides was maintained in the range of 0.1×10^{-4} M to 100×10^{-4} M. All the reactions were initiated by adding required amount of oxo(salen) complex to a thermally equilibrated mixture of PSAA and LO in acetonitrile in such a way that in each run the total volume was 3 ml. The kinetics of the reaction was followed by measuring the decay in absorbance of the oxo(salen)chromium(V)$^{+}$-LO-PSAA adduct with time at the appropriate wavelength (Table 1). The representative kinetic run showing the decrease in the absorbance value of oxo(salen)chromium (V)$^{+}$-LO-PSAA adduct during its reaction with PSAA in the presence of ligand oxide is shown in Fig. 2.

3.3. Dependence of reaction rate on reactants

The dependence of the reaction rate on PSAA in the presence of three ligand oxides namely TPPO, PyO, PicNO is studied by measuring the rate at different [PSAA] in the range from 0.05 M to 0.4 M. The rate constants calculated from the pseudo-first-order plots at different concentrations of PSAA are recorded in Supporting information Table S1 which indicates that an increase in PSAA concentration increases the k_1. However, the non-integral slope value observed in the plots of $\log k_1$ vs. log [PSAA] with different ligand oxides supports the fractional-order dependence of PSAA. The order observed with PSAA from the double logarithmic plot of k_1 and [PSAA] for different combinations are given in Supporting information Table S2. Again the plots of k_1 against [PSAA] (Fig. 3) and $1/k_1$ against 1/[PSAA] are found to be linear with specific intercept in the y-axis confirm the fractional order dependence on PSAA.

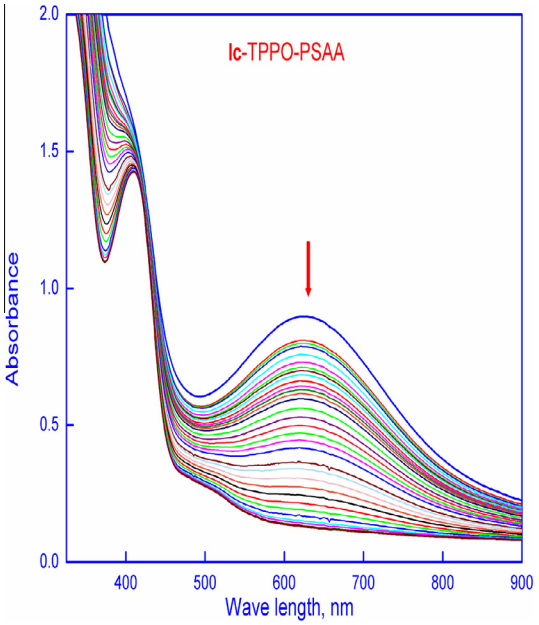

Fig. 2. The absorption spectral change with time for the reaction between PSAA and **Ic** in the presence of TPPO. [PSAA] = 2×10^{-1} M; [**Ic**] = 5×10^{-4} M; [TPPO] = 1×10^{-2} M.

The observed linear pseudo-first-order plots and the constant pseudo-first-order rate constants calculated at different initial concentrations of oxo(salen)Cr(V)$^{+}$ ions (Supporting information Table S1) show the first-order kinetics of the reaction with respect to oxo(salen)Cr(V)$^{+}$. The observed trend of constant k_1 with varying [oxo(salen)Cr(V)$^{+}$] is contradictory with that observed for the reactions in the absence of ligand oxides and in the presence of nitrogen bases [34] where decrease in k_1 with concentration is noted.

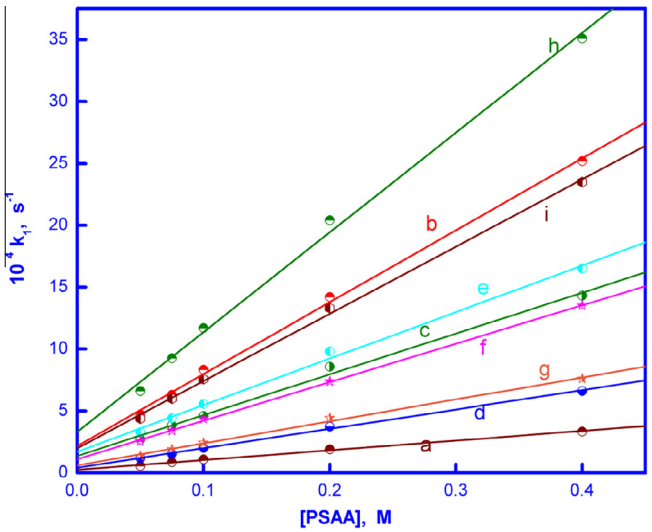

Fig. 3. Plots of k_1 vs. [PSAA] for the reactions. a, **Ia** with TPPO; b, **Ia** with PyO; c, **Ia** with PicNO; d, **Ib** with TPPO; e, **Ib** with PyO; f, **Ib** with PicNO; g, **Ic** with TPPO; h, **Ic** with PyO; i, **Ic** with PicNO. General conditions are as in Table 3.

This indicates that oxo(salen) dimer formation is prevented by ligand oxides.

From the Supporting information Table S1 it is inferred that the rate of the reaction is influenced by the nature of the substituents in the salen ligand. Electron-withdrawing chloro substituent in 5,5′-positions of oxo(salen) complex increases the rate constant of the reaction while electron-releasing methyl substituent in the 5,5′-positions slightly reduces the reaction rate except with TPPO (where rate acceleration is observed) when compared to that of the unsubstituted oxo(salen) complex. Thus the observed order of reactivity among the oxo(salen)chromium(V)$^+$ complexes in the presence of ligand oxide is oxo(5,5′-$(CH_3)_2$salen) < unsubstituted < oxo(5,5′-Cl_2salen).

Further, the overall rate constant (k_{ov}) calculated by dividing the pseudo-first-order rate constant by $[PSAA]^{order}$ appears to be a constant for a particular oxo complex (Supporting information Table S1). From the above results and observation, it is concluded that the order with respect to PSAA is fractional and the reactions of PSAA with oxo(salen)Cr(V)$^+$ ion proceed through Michaelis–Menten kinetics in the presence of ligand oxides. The Michaelis–Menten constants (K_M) calculated from the slope and intercept values of the linear $1/k_1$ vs. 1/[PSAA] plots are given in Table S3. The data in Table S3 indicate that K_M value is not sensitive to the change of substituents in the salen ligand and the nature of ligand oxides. The increase in pseudo-first-order rate constant with increase in [PSAA] without saturation even at high PSAA concentrations and relatively high value of K_M prove that the binding of PSAA with the active species of oxo(salen)Cr(V)$^+$ ion is weak in nature.

3.4. Effect of ligand oxides on the reaction rate

The influence of ligand oxides on the reaction rate is studied by varying the concentrations of TPPO, PyO and PicNO over the range of 0.50×10^{-3} M and 100×10^{-3} M. The reactions could not be carried out at higher concentrations as they are too fast to be measured or the oxo(salen) complex undergoes some sort of decomposition which is shown by decrease in absorbance. The calculated pseudo-first-order and overall rate constant values at various ligand oxide concentrations for different combinations of oxo (salen)Cr(V)$^+$ ions and ligand oxides are presented in Supporting information Table S4.

It is inferred from the data that all the ligand oxides studied have strong influence on rate acceleration with all the three oxo (salen) complexes. The observed order of reactivity among the ligand oxides is PicNO > PyO > TPPO. One interesting observation noted in the ligand oxide catalyzed reactions is the saturation kinetics observed in TPPO with complex **Ib**. Though TPPO shows catalytic effect with complexes **Ia** and **Ic** and the reactions of complex **Ib** get accelerated by PyO and PicNO without any saturation, the reaction of PSAA with complex **Ib** and TPPO attained a saturation in rate constant even from the lowest concentration.

Linear plots of $\log k_1$ vs. log [LO] with non-integral slope values for the data in Supporting information Table S4 indicate the fractional-order dependence and operation of Michaelis–Menten kinetics with respect to ligand oxide. Michaelis–Menten constants calculated from the double reciprocal plots of k_1 and [LO] are tabulated in Supporting information Table S3. The appreciable low Michaelis–Menten constants clearly show that binding between LOs and complexes are strong in nature.

3.5. Substituent effects

In order to study the effect of substituents in the oxidative decarboxylation, the reactivity of ten *para*- and *meta*-substituted PSAAs with oxo(salen)Cr(V)$^+$ ions (**Ia**–**Ic**) were studied in the presence of TPPO, PyO and PicNO. The overall rate constants calculated for the reactions in the presence of ligand oxides are tabulated in Table 3. The kinetic data in the table indicate that the reactions in the presence of ligand oxides are highly sensitive to the nature of the substituents in the aryl moiety of PSAA and in the phenolic part of the salen ligand. Both electron-withdrawing and electron-donating substituents in the phenyl ring of PSAA increase the rate of the reaction. In order to confirm the extent of charge separation in the transition state, the rate constant values were analyzed in terms of Hammett σ values. V-shaped Hammett plots with a minimum for unsubstituted PSAA are seen with all ligand oxides and oxo(salen) complexes. The Hammett plots are found to have positive ρ value for electron-withdrawing substituents ($\rho^+ = 0.057$ to 0.886) and negative ρ value for electron-releasing substituents ($\rho^- = -0.740$ to -4.10). The representative Hammett plots are shown in Fig. 4. Regarding the substituent effect in salen complex, the electron-withdrawing chloro substituent in the 5,5′ positions of the salen ligand (**Ic**) enhances the rate enormously while the electron-donating methyl substituent (**Ib**) decreases the rate which is slightly lower than the unsubstituted oxo(salen) complex (**Ia**). This is in accordance with the low binding constant value observed in 5-Me substituted oxo(salen) complex with the ligand oxides.

3.6. Effect of temperature and activation parameters

In order to calculate the thermodynamic parameters, the kinetics of the reaction between PSAA and **Ia** is followed at three different temperatures in the range 298 K–313 K in the presence of added ligand oxides. The overall rate constants and the thermodynamic parameters calculated using Eyring's plot of log (k_{ov}/T) against $1/T$ (Supporting information Fig. S6) are given in Supporting information Table S5. The obtained positive value of enthalpy of activation, $\Delta^{\ddagger}H$ reflects endothermic nature of the reaction. The negative entropy of activation, $\Delta^{\ddagger}S$ values indicate the involvement of highly structured transition state in the mechanism. The observed constant $\Delta^{\ddagger}H$ (66.0 to 77.2 kJ mol^{-1}) and $\Delta^{\ddagger}S$ (-54.6 to -81.0 J K^{-1} mol^{-1}) values in the presence of different ligand oxides not only indicate the operation of same mechanism with all ligand oxides and also proves that the reactions are neither enthalpy controlled nor entropy controlled.

Table 3
Overall rate constants for the oxidative decarboxylation of PSAAs by **Ia–Ic** in the presence of ligand oxides.

X-PSAA	$10^4\ k_{ov}$, $(M^{-1})^n\ s^{-1}$								
	(**Ia**)			(**Ib**)			(**Ic**)		
	TPPO	PyO	PicNO	TPPO	PyO	PicNO	TPPO	PyO	[a]PicNO
p-OMe	49.1 ± 0.83	82.9 ± 2.5	76.3 ± 0.30	57.8 ± 0.24	79.6 ± 0.18	65.9 ± 0.67	109 ± 8.9	119 ± 9.7	244 ± 3.1
p-OEt	36.0 ± 1.3	79.8 ± 0.61	56.6 ± 1.9	43.4 ± 2.0	60.0 ± 0.73	54.1 ± 1.1	86.7 ± 2.7	105 ± 7.5	148 ± 14
p-Me	14.4 ± 0.25	60.2 ± 1.6	56.5 ± 0.59	28.0 ± 1.0	48.5 ± 1.5	50.7 ± 1.2	31.4 ± 0.77	90.0 ± 2.7	110 ± 1.0
m-Me	8.37 ± 0.15	50.0 ± 2.3	46.2 ± 0.63	15.4 ± 0.27	42.2 ± 1.9	40.8 ± 4.4	17.6 ± 0.49	79.0 ± 6.8	65.0 ± 1.2
H	7.43 ± 0.40	51.7 ± 1.2	30.0 ± 1.6	14.7 ± 0.51	35.2 ± 0.48	27.4 ± 0.81	16.4 ± 0.49	73.4 ± 3.1	48.1 ± 2.4
p-F	8.69 ± 0.18	50.3 ± 0.50	30.4 ± 0.28	15.2 ± 0.16	37.0 ± 0.14	29.2 ± 0.15	17.1 ± 0.42	80.5 ± 0.39	50.8 ± 1.1
p-Cl	11.4 ± 1.7	52.1 ± 2.6	32.4 ± 0.34	17.8 ± 0.45	38.5 ± 3.2	29.9 ± 1.1	21.2 ± 0.28	95.2 ± 0.51	53.1 ± 1.3
m-F	12.9 ± 0.77	53.6 ± 0.76	33.4 ± 1.9	25.9 ± 0.48	41.0 ± 1.8	32.8 ± 0.58	27.0 ± 1.1	130 ± 4.9	52.9 ± 0.75
m-Cl	14.6 ± 0.23	54.3 ± 0.16	34.5 ± 0.13	20.0 ± 0.47	40.2 ± 3.3	34.3 ± 0.43	33.1 ± 0.75	131 ± 0.48	54.0 ± 0 .28
p-NO_2	25.8 ± 2.5	56.1 ± 2.0	49.8 ± 1.2	51.2 ± 1.6	52.5 ± 2.9	47.8 ± 1.6	76.7 ± 1.4	172 ± 11	58.6 ± 6.8
ρ^-=	−3.12 ± 0.52	−1.16 ± 0.15	−1.24 ± 0.26	−2.27 ± 0.29	−1.15 ± 0.20	−1.23 ± 0.19	−4.10 ± 0.60	−0.740 ± 0.10	−2.42 ± 0.28
(r=)	(0.961)	(0.985)	(0.939)	(0.976)	(0.956)	(0.965)	(0.980)	(0.975)	(0.981)
ρ^+=	0.655 ± 0.03	0.057 ± 0.01	0.308 ± 0.04	0.751 ± 0.12	0.214 ± 0.02	0.303 ± 0.03	0.886 ± 0.07	0.491 ± 0.07	0.084 ± 0.01
(r=)	(0.997)	(0.934)	(0.972)	(0.966)	(0.982)	(0.981)	(0.989)	(0.961)	(0.985)

[TPPO] = 1.0×10^{-2} M; [PyO] = 5.0×10^{-3} M; [PicNO] = 1.0×10^{-3} M. [**Ia**] = [**Ib**] = [**Ic**] = 5.0×10^{-4} M.
[a] For (**Ic**) [PicNO] = 5.0×10^{-4} M; Temp. = 303 K; solvent = 100% CH_3CN; *n* = order w.r.t. PSAA.

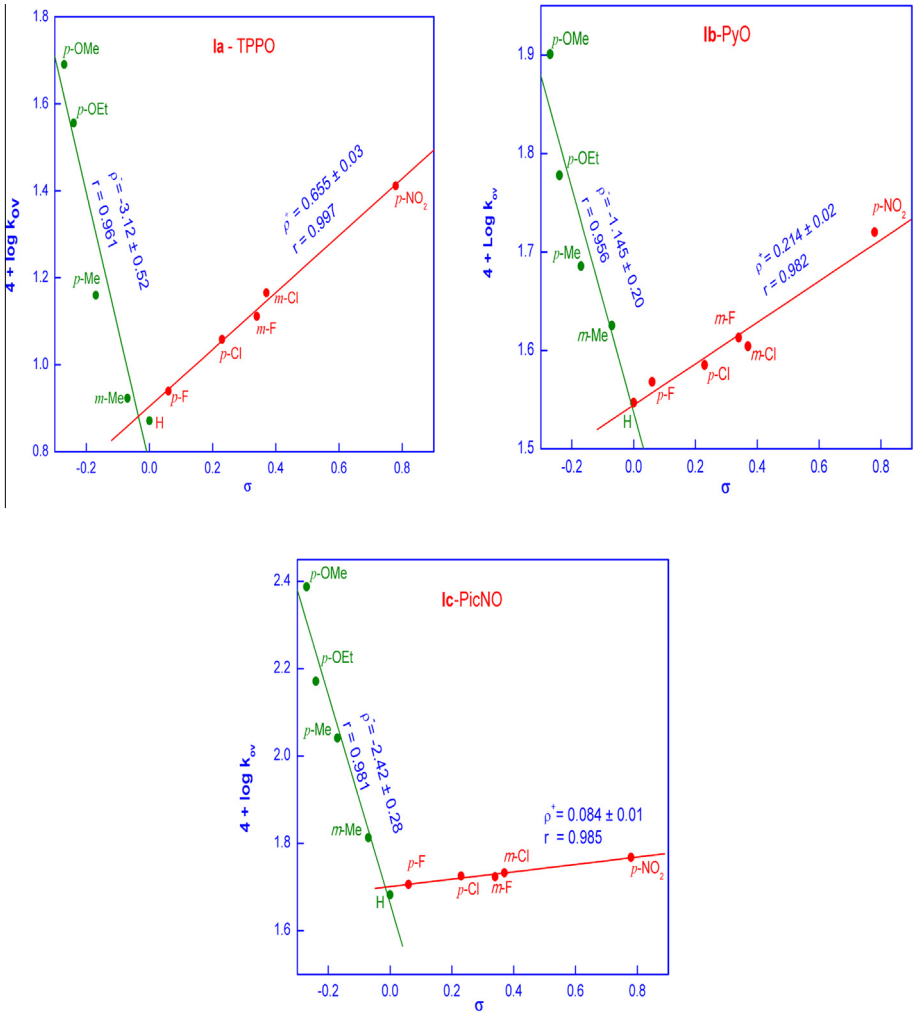

Fig. 4. Hammett plots for the substituent variation in PSAA in the presence of ligand oxides.

3.7. Discussion

The observed spectral changes involving enormous red shift in λ_{max} value, significant increase in absorbance value and the existence of an isobestic point in the absorption spectral titrations with different concentrations of LOs (Fig. 1) along with the visible color change during the addition of LO to oxo(salen)Cr(V)$^+$ ion unambiguously confirm the formation of 1:1 adduct between LO and

oxo(salen) complex in a reversible process. Strong binding of LOs with the complex during adduct formation is confirmed from the larger binding constant values (Table 2) and smaller Michaelis–Menten constants observed with LOs (Table S3). In many salen mediated oxidation reactions, the LO-salen adduct formed during the course of the reaction has been proposed as the active oxidizing species and it is proved to be a more powerful oxidant than the salen complex itself. The catalytic activity shown by the added ligand oxides is 2–70 times (Table S4) greater than that in its absence. This confirms the involvement of oxo(salen)$Cr(V)^{+}$-LO adduct as the active reactive species in the present reaction series also.

Ligand oxides are reported to co-ordinate with the Cr centre through the oxygen atom in the apical centre to complete the octahedral co-ordination which weakens the Cr=O bond, increasing the bond length by donating electron density into the Cr=O anti bonding orbital [53,54]. The rate enhancement observed in the presence of N-oxides is in line with the increase in rate observed in the sulfoxidation [55,56] and epoxidation reactions by oxo(salen)$Cr(V)^{+}$ [57–60] and oxo(salen)Mn(V) [61] complexes. Additive like 4-phenylpyridine N-oxide (4-PPNO) facilitates faster reaction rates, higher epoxide yields and improved enantio-selectivity [61–67] in the Mn(III) salen mediated reactions. On the other hand in the epoxidation of olefins [53] and in the oxidation of aryl methyl sulfides [29,68], aryl phenyl sulfides [30,69], sulfoxides [31,32] and arylthioacetic acids [33] by oxo(salen)manganese(V) complexes, the added LOs have no appreciable effect on the reaction rate.

From the kinetic data in Tables 3, S1 and S2 it is shown that the reactivity is more pronounced in the presence of added PyO and PicNO while it is not so with added TPPO. This is a striking contrast to the order of catalysis observed with LOs in the oxygenation of organic sulfides and sulfoxides by oxo(salen)$Cr(V)^{+}$ ion [55,56] where highest reactivity is observed with TPPO. The low binding constant values and least reactivity observed with TPPO among the LOs in this reaction series may be attributed not only to the steric hindrance created by TPPO during the binding with chromium centre [70] but also due to decrease in electron density on the oxygen atom of TPPO as a result of the presence of three electron-withdrawing phenyl groups. These effects decelerate the formation of oxo(salen)-TPPO reactive adduct species. Earlier studies [28,45] revealed that TPPO adduct with oxo(salen)$Cr(V)^{+}$ ions are less stable than PyO adduct. In the computational assessment of donor ligand effect on the product distribution in the manganese (salen) catalyzed epoxidation of olefins, Jacobsen et al. [71] have shown that PyO forms a stronger bond with the transition metal centre than TPPO. Gilheany et al. [17] reported that bulky ligands are less effective donor ligands and their rate of donor ligation is lower than expected. The binding constant values in Table 2 reveal that the PyO forms stronger adduct with oxo(salen)$Cr(V)^{+}$ ions. The unusual high binding constants of PyO has been attributed to the dual nature of the N-oxide group which acts both as an electron-donor and an electron-acceptor [72,73].

The observed higher reactivity in the presence of PicNO than with PyO may be due to the existence of methyl group in the *para*-position of the pyridine ring which increases the electron density on oxygen of PicNO. Though the binding constant between oxo(salen) and PyO is higher than with PicNO the presence of methyl group in PicNO favors the easy formation of oxo(salen)-PicNO adduct which is the active species necessary for a reaction to proceed. These findings together with lower reactivity in TPPO confirm the existence of correlation between the order of catalytic activity and the donor ability of the LOs, suggesting the importance of electronic effect.

On the basis of the foregoing argument it is concluded that the first step in the mechanism (Scheme 2) is the formation of 1:1 adduct ($\mathbf{C_1}$) between oxo(salen) complex and LO in a reversible step which is the active oxidant. From the fractional-order dependence on PSAA and the observed high Michaelis-Menten constants, it is assumed that in the second step of the mechanism PSAA binds in a weak manner with $\mathbf{C_1}$ to form a ternary complex ($\mathbf{C_2}/\mathbf{C_3}$) in a reversible step. The spectral evidence for the formation of $\mathbf{C_2}/\mathbf{C_3}$ is the change in the absorbance and λ_{max} value (Table 1) of the oxo(salen) complex-LO adduct by the addition of PSAA. From the density functional theory (DFT) it was calculated that the co-ordination of donor ligands with oxo(salen)$Cr(V)^{+}$ ions lowers the energy of activation [12,13] during the addition of alkene to oxo(salen)$Cr(V)^{+}$ which explains the increase in rate noted in the epoxidation reactions with donor ligand as additive.

Further, the axial ligands with strong binding ability have a profound effect on the conformation of the basal salen ligand. The metal centre, which is positioned above the plane of the four basal hetero atoms in oxo salen [45], moves into the plane and the salen ligand is slightly distorted towards a step like transoid conformation when donor ligand is coordinated [74] which favors the attack of a substrate. Bahraoui et al. [75] have shown experimentally that axial coordination of N-oxide ligand to the oxo(salen)-manganese (V) complex raises the catalytic activity and the oxygen transfer dramatically. Thus it is proposed that one of the reasons for the observed significant rate acceleration in the presence of ligand oxides is the favorable condition for the binding of PSAA with oxo oxygen of the salen moiety.

The Hammett correlations of reactivity of different *para*- and *meta*-substituted derivatives of PSAA with complexes **Ia**–**Ic** in the presence of LOs reveal V-shaped plots (Fig. 4). Similar non-linear Hammett plots have been observed in the oxidation of substituted benzaldehyde by quinolinium chlorochromate [76], thioether substrates by manganese(V) corrolazine complex [77], trans cinnamic acid by pyridinium chlorochromate [78] and by chloramine T [79], styrene derivatives by quaternary ammonium permanganate [80], sulfoxidation by titanium complex [81] and H-atom transfer reaction in *p*-substituted 2,6-di(t-Bu)phenol by manganese^{V}(imido)(-corrole) complex [82] etc. Such type of non-linear upward Hammett plots have been interpreted by a distinct change in reaction mechanism or free radical mechanism [77,82,83].

In the oxidation of alcohols by ruthenate and perruthenate ions [84] the appearance of concave upward Hammett plot was explained by the involvement of free radical like transition state. In the Cr(VI) oxidation of benzylamines [85] the observed U-shaped Hammett plot was indicated by a change in the relative importance of bond formation and bond fission in the transition state. Because of the competition between the rate of complex formation by electron-releasing groups and its rate of decomposition by electron-withdrawing groups, V-shaped Hammett plots are seen in the oxidation of benzaldehydes by quinolinium chlorochromate [76]. V-shaped Hammett plots observed in manganese(V) oxo (corrolazine) [77] and manganese^{V}(imido)(corrole) [82] complexes were rationalized based upon a change in mechanism that hinges the complexes to function as either an electrophile or nucleophile. In the present system too the V-shaped Hammett plot is indicative of a change in mechanism.

In Fig. 4 electron-donating substituents show a good linear correlation with an expected negative slope (ρ^{-}) which can be successfully explained by the mechanism involving electrophilic attack of the oxo(salen)chromium(V)$^{+}$-LO adduct ($\mathbf{C_1}$) on the sulfur centre of PSAA. The observed negative reaction constant (ρ^{-}) indicates the accumulation of positive charge at the sulfur centre while the magnitude of ρ^{-} indicates the extent of charge development on the sulfur centre in the transition state. The appreciably high ρ^{-} values obtained indicate that electron-releasing substituents in PSAA create more positive charge on the sulfur atom and thus increase the nucleophilicity of PSAA. Another reason for the high

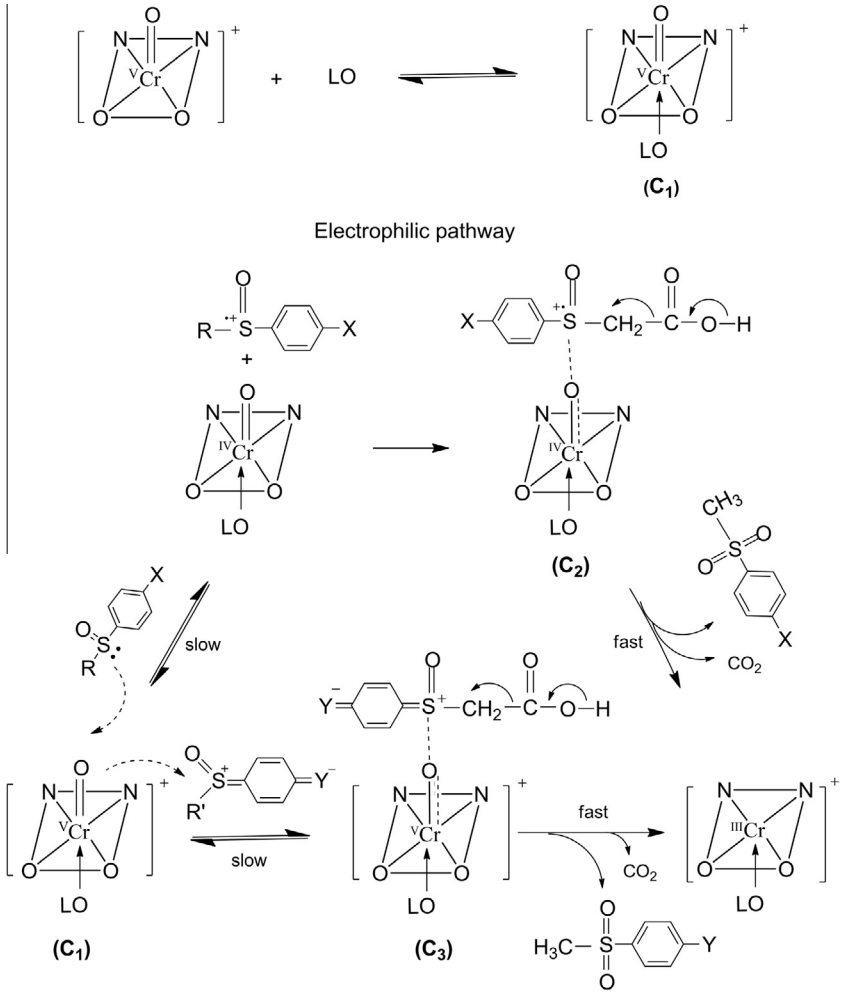

X = electron donating group ; Y = electron withdrawing group ;
R = CH_2COOH ; LO = TPPO, PyO, PicNO

Scheme 2. Possible electrophilic and nucleophilic pathways.

ρ value may be due to significant increase in electrophilic character of the ligand oxide coordinated octahedral oxo(salen)chromium $(V)^+$ adduct. Also the DFT studies on sulfoxidation by oxo(salen)Cr $(V)^+$ ions made by Venkataramanan et al. [56] indicated an increase in negative charge over chromium atom in the transition state. A negative ρ value was already reported for a series of sulfoxidation reactions with oxo(salen)Cr$(V)^+$ ion [55]. An interesting observation noted in the present study is that the $\log k_{ov}$ values are linearly related with the oxidation potential of various substituted PSAAs when electron-donating groups are present, while linearity is not observed with electron-withdrawing substituents. The plots of $\log k_{ov}$ vs. E_{ox} are shown in Fig. 5.

Linear correlation is expected between $\log k_2$ and E_{ox}/E_{red} for a single-electron transfer process (SET). The observed linear plots of $\log k_{ov}$ vs. E_{ox} along with negative ρ value obtained in the Hammett correlation for electron-releasing substituents give direct evidence for the electrophilic attack of the oxo complex on PSAA involving single-electron transfer from the sulfur atom to the oxidant species. This step involves the formation of sulfur cation radical and this would be the slow rate determining step. Such type of sulfur cation radical formation in a rate determining step is firmly established in literature. Sulfur cation radical then

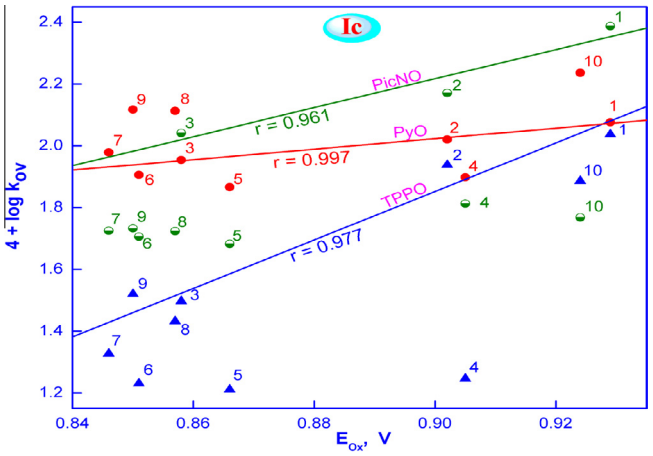

Fig. 5. Log k_{ov} vs. E_{ox} plot for the reaction of PSAA with **Ic** in the presence of ligand oxides. The numbers are in the order *p*-OMe, *p*-OEt, *p*-Me, *m*-Me, H, *p*-F, *p*-Cl, *m*-F *m*-Cl and *p*-NO_2.

undergoes several fast steps including oxygen transfer (OT) from the oxo function of the complex to PSAA and decarboxylation from PSAA moiety by α, β-cleavage leading to the formation of the products, methyl phenyl sulfone and CO_2 for PSAAs having electron-releasing groups. It is pertinent to mention here that on the basis of the observed linear correlation of $\log k_2$ and E_{red}, SET mechanism has been proposed for the sulfoxidation of PTAA [33] and sulfides [31,68] by oxo(salen)Mn(V) complexes, and oxidation of anilines by oxo(salen)Cr(V)$^+$ [47] and oxo(salen)iron(IV) [23] complexes.

The observed positive reaction constant (ρ^+) for electron withdrawing substituents in the Hammett plot indicates a change in mechanism for PSAAs with such substituents. A possible explanation for the increase in rate by electron-withdrawing substituents comes from the existence of quinonoid type resonance structures shown in Fig. 6 which may be partly stabilized by electron-withdrawing substituents.

The evidence for the contribution of a similar quinonoid type resonance form in organic sulfur compounds containing electron-withdrawing substituents is recently advocated by Nakazawa et al. [86] and Neu et al. [77]. As a result of generation of partial positive charge on the sulfur atom, PSAAs with electron-withdrawing groups become electrophilic in character. In such cases, the hexa coordinated oxo(salen)-LO adducts which behave as electrophiles with PSAAs containing electron-donating substituents now act as nucleophiles and facilitate the formation of intermediate C_3 in a slow reversible rate determining step which then undergoes decarboxylation and decomposition to give [(salen)Cr(III)-LO]$^+$, CO_2 and sulfone as the products in a fast step. Such type of sulfonium ion formation between oxo(salen)Cr(V)$^+$ ion and sulfur compounds in a slow step has been advocated earlier in many sulfoxidation reactions of sulfides and sulfoxides [55,56,87].

The quinonoid type resonance structure of PSAA containing electron withdrawing substituents can enhance the rate of S–O bond formation in the intermediate (**C_3**) followed by transfer of oxygen to PSAA. These are facilitated further more with the increase in electron-withdrawing power of the substituents and accounts for the observed positive ρ value with electron withdrawing substituents in PSAA. In contrast, the electron-donating substituents exhibit negligible contribution for the formation of **C_3** because of their high electron density on sulfur atom. Thus the observed substituent effect and V-shaped Hammett plot are rationalized on the basis of change in mechanism that hinges the oxo(salen)Cr(V)$^+$ ion to function either as an electrophile or nucleophile depending upon the nature of substituents in PSAA. The two possible mechanistic scenarios, electrophilic and nucleophilic attack of oxo(salen)-chromium(V) with PSAA are shown in Scheme 2.

The liberation of CO_2 during the course of the reaction was confirmed using the method reported by Crossno et al. [88]. IR, LC–MS and GC–MS spectra confirm the formation of methyl phenyl sulfone. The IR spectrum of the product is found to have characteristic SO_2 stretching frequencies at 1148 cm^{-1} and 1290 cm^{-1}. The GC–MS analysis of the product indicates a peak corresponding to m/z = 156 which authenticate the formation of methyl phenyl sulfone as the only product under the experimental conditions. The peak eluted in LC–MS at a retention time of 1.87 min ionizes in APCI (+) mode corresponds to a mass of 157 also conforms that methyl phenyl sulfone is the only product formed in the reaction. The absorption spectrum of the inorganic product formed during the reaction is identical with that of Cr^{III}(salen) spectrum.

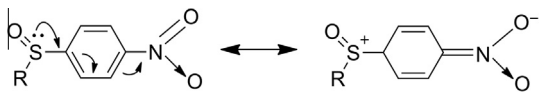

Fig. 6. Resonance structures for electron-withdrawing substituents.

In order to gain additional evidence for the operation of different mechanisms in different substituted PSAAs and to test the applicability of reactivity-selectivity principle (RSP) in the present system, the k_2 values (Table 3) for the reactions of different substituted PSAAs with oxo(salen)Cr(V)$^+$ ions (**Ia–Ic**) in the presence of ligand oxides are subjected to a mathematical treatment formulated by Exner [89] using Eq. (2).

$$\log k_{Fi} = a + b \log k_{Si} + \varepsilon_i \quad (2)$$

In the present system no linear correlation is observed between logarithms of rate constants of fast reaction (k_{Fi}) versus slow reaction (k_{Si}). The observed results not only show the non-applicability of RSP in the presence of ligand oxides but also confirm the operation of different mechanisms in different substituted PSAAs as proposed in Scheme 2 for electron-donating and electron-withdrawing substituents.

4. Conclusions

Since decarboxylation process play an important role in different areas of organic synthesis as well as in biochemical reactions and N-oxides of heterocyclic amines play important role in the reactions leading to the modification of enzymes and biological reductive systems, the oxidative decarboxylation of several phenylsulfinylacetic acids by oxo(salen)Cr(V)$^+$ ions in the presence of ligand oxides have been investigated in acetonitrile. The effect of additives like ligand oxides on the reactivity showed an accelerating effect. The order of catalytic activity of ligand oxides, PicNO > -PyO > TPPO has been explained on the basis of electron density on oxygen and relative ability of binding of LO with oxo(salen)Cr(V)$^+$ ion. The observed nonlinear substituent effect in the Hammett plot has been rationalized by change in mechanism from single electron transfer to S_N2 type reaction upon changing the substituents in PSAA from electron-donating to electron withdrawing. Thus the study of reactivity of oxo(salen)Cr(V)$^+$ ion in the presence of different N-oxides establish a more efficient biomimetic catalyst system for the catalytic oxidative decarboxylation of aromatic acids.

Acknowledgement

Financial support from University Grants Commission (UGC), India in the form of a major research project (F.No.39-817/2010 (SR) to PS is gratefully acknowledged. SSD is thankful to UGC, SERO, Hyderabad and Manonmaniam Sundaranar University, Tirunelveli for awarding teacher fellowship (No.F.ETFTNMS045) under FDP. The authors are extremely thankful to the management of Aditanar College of Arts and Science, Tiruchendur for providing facilities.

Appendix A. Supplementary data

Supplementary data associated with this article can be found, in the online version, at http://dx.doi.org/10.1016/j.poly.2016.05.012.

References

[1] T. Katsuki, Coord. Chem. Rev. 140 (1995) 189.
[2] L. Canali, D.C. Sherrington, Chem. Soc. Rev. 28 (1999) 85.
[3] C.T. Dalton, K.M. Ryan, V.M. Wall, C. Bousquet, D.G. Giheany, Top. Catal. 5 (1998) 75.
[4] P.G. Cozzi, Chem. Soc. Rev. 33 (2004) 410.
[5] J.F. Larrow, E.N. Jacobsen, Top. Organomet. Chem. 6 (2004) 123.
[6] C.T. Cohen, T. Chu, G.W. Coates, J. Am. Chem. Soc. 127 (2005) 10869.
[7] H. Groger, Chem. Rev. 103 (2003) 2795.
[8] G.M. Sammis, E.N. Jacobsen, J. Am. Chem. Soc. 125 (2003) 4442.
[9] W. Sun, H. Wang, C. Xia, J. Li, P. Zhao, Angew. Chem., Int. Ed. 42 (2003) 1042.
[10] G.M. Sammis, H. Danjo, E.N. Jacobsen, J. Am. Chem. Soc. 126 (2004) 9928.
[11] S.X. Wang, M.X. Wang, D.X. Wang, J. Zhu, Angew. Chem., Int. Ed. 47 (2007) 388.

[12] S.R. Doctrow, K. Huffman, C.B. Marcus, G. Tocco, E. Malfroy, C.A. Adinolfi, H. Kruk, K. Baker, N. Lazarowych, J. Mascarenhas, B. Malfroy, J. Med. Chem. 45 (2002) 4549.
[13] M. Baudry, S. Etienne, A. Bruce, M. Palucki, E. Jacobsen, B. Malfroy, Biochem. Biophys. Res. Commun. 192 (1993) 964.
[14] J. Balzarini, E. Keyaerts, L. Vijgen, F. Vandermeer, M. Stevens, E. De Clercq, H. Egberink, M. Van Ranst, J. Antimicrob. Chemother. 57 (2006) 472.
[15] A. Albini, S. Pietra, Heterocyclic N-oxides, CRC Press, Boca Raton, 1991.
[16] B. Ganley, G. Chowdhury, J. Bhansali, J. Scott Daniels, K.S. Gates, Bioorg. Med. Chem. 9 (2001) 2395.
[17] E.M. McGarrigle, D.G. Gilheany, Chem. Rev. 105 (2005) 1564.
[18] M. Bagherzadeh, R. Latifi, L. Tahsini, J. Mol. Catal. A: Chem. 260 (2006) 163.
[19] M. Bagherzadeh, L. Tahsini, R. Latifi, Catal. Commun. 9 (2008) 1600.
[20] D. Mohajer, L. Sadeghian, J. Mol. Catal. A: Chem. 272 (2007) 191.
[21] A. Ghaemi, S. Rayati, S. Zakavi, N. Safari, Appl. Catal. A 353 (2009) 154.
[22] D.J. Darensbourg, A.I. Moncada, W. Choi, J.H. Reibenspies, J. Am. Chem. Soc. 130 (2008) 6523.
[23] A.M. Aslam, S. Rajagopal, M. Vairamani, M. Ravikumar, Transition Met. Chem. 36 (2011) 751.
[24] A. Chellamani, N.M.I. Alhaji, S. Rajagopal, J. Phys. Org. Chem. 20 (2007) 255.
[25] B. Bahramian, V. Mirkhani, S. Tangestaninejad, M. Moghadam, J. Mol. Catal. A: Chem. 244 (2006) 139.
[26] A. Chellamani, P. Sengu, N.M.I. Alhaji, J. Mol. Catal. A: Chem. 317 (2010) 104.
[27] P. Subramaniam, T. Vanitha, T. Kodispathi, C. Shanmuga Sundari, J. Mex. Chem. Soc. 58 (2014) 211.
[28] K. Srinivasan, S. Perrier, J.K. Kochi, J. Mol. Catal. A: Chem. 36 (1986) 297.
[29] A. Chellamani, S. Harikengaram, J. Phys. Org. Chem. 16 (2003) 589.
[30] A. Chellamani, S. Harikengaram, Helv. Chim. Acta 94 (2011) 453.
[31] A. Chellamani, P. Kulanthaipandi, S. Rajagopal, J. Org. Chem. 64 (1999) 2232.
[32] A. Chellamani, S. Harikengaram, J. Mol. Catal. A: Chem. 247 (2006) 260.
[33] A. Chellamani, P. Sengu, J. Mol. Catal. A: Chem. 283 (2008) 83.
[34] P. Subramanim, S. Sugirtha Devi, S. Anbarasan, J. Mol. Catal. A: Chem. 390 (2014) 159.
[35] P. Subramaniam, N. ThamilSelvi, S. Sugirtha Devi, J. Korean Chem. Soc. 58 (2014) 17.
[36] P. Subramaniam, N. ThamilSelvi, J. Serb. Chem. Soc. 80 (2015) 1.
[37] P. Subramaniam, N. ThamilSelvi, Am. J. Anal. Chem. 4 (2013) 20.
[38] P. Subramaniam, N. ThamilSelvi, Bull. Chem. Soc. Ethiop. 30 (2016) 137.
[39] C. Shibuya, H. Itoh, Y. Usubuchi, M. Akamine, US patent US 4245107 A, 1981.
[40] K. Lee, Bull. Korean Chem. Soc. 32 (2011) 3477.
[41] A.A. Jaxa-Chamiec, P.G. Sammes, P.D. Kennewell, J. Chem. Soc. Perkin Trans. 1 (1980) 170.
[42] Q.B. Cass, A.A. Jaxa-Chamiec, P.G. Sammes, P.D. Kennewell, J. Chem. Soc., Chem. Commun. 24 (1981) 1248.
[43] Z. Zhang, M. Bao, B. Liu, Hechang Huaxue 10 (2002) 241.
[44] T. Allmendinger, Tetrahedron 47 (1991) 4905.
[45] K. Srinivasan, J.K. Kochi, Inorg. Chem. 24 (1985) 4671.
[46] E.M. McGarrigle, D.M. Murphy, D.G. Gilheany, Tetrahedron Asymmetry 15 (2004) 1343.
[47] S. Premsingh, N.S. Venkataramanan, S. Rajagopal, S.P. Mirza, M. Vairamani, P. Rao, K. Velavan, Inorg. Chem. 43 (2004) 5744.
[48] D.J. Pasto, D. Mcmillen, T. Murphy, J. Org. Chem. 30 (1965) 2688. and references cited therein.
[49] K.B. Shaw, R.K. Miller, Can. J. Chem. 48 (1970) 1394.
[50] H.D. Crockford, T.B. Douglas, J. Am. Chem. Soc. 56 (2002) 1472.
[51] H.A. Benesi, J.H. Hildebrand, J. Am. Chem. Soc. 71 (1949) 2703.
[52] W.B. Person, J. Am. Chem. Soc. 87 (1965) 167.
[53] K. Srinivasan, P. Michaud, J.K. Kochi, J. Am. Chem. Soc. 108 (1986) 2309.
[54] T.L. Siddall, N. Miyaura, J.C. Huffman, J.K. Kochi, J. Chem. Soc., Chem. Commun. (1983) 1185.
[55] N.S. Venkataramanan, S. Premsingh, S. Rajagopal, K. Pitchumani, J. Org. Chem. 68 (2003) 7460.
[56] N.S. Venkataramanan, S. Rajagopal, Tetrahedron 62 (2006) 5645.
[57] N.J. Kerrigan, I.J. Langan, C.T. Dalton, A.M. Daly, C. Bousquet, D.G. Gilheany, Tetrahedron Lett. 43 (2002) 2107.
[58] C.T. Dalton, K.M. Ryan, I.J. Langan, E.J. Coyne, D.G. Gilheany, J. Mol. Catal. A: Chem. 187 (2002) 179.
[59] A.M. Daly, D.G. Gilheany, Tetrahedron Asymmetry 14 (2003) 127.
[60] A.M. Daly, M.F. Renehan, D.G. Gilheany, Org. Lett. 3 (2001) 663.
[61] J.P. Collman, L. Zeng, J.I. Brauman, Inorg. Chem. 43 (2004) 2672.
[62] N.S. Finney, P.J. Pospisil, S. Chang, M. Palucki, R.G. Konsler, K.B. Hansen, E.N. Jacobsen, Angew. Chem., Int. Ed. Engl. 36 (1997) 1720.
[63] M. Palucki, P.J. Pospisil, W. Zhang, E.N. Jacobsen, J. Am. Chem. Soc. 116 (1994) 9333.
[64] R. Irie, Y. Ito, T. Katsuki, Synlett (1991) 265.
[65] K. Miura, T. Katsuki, Synlett (1999) 783.
[66] P. Pietikainen, Tetrahedron Lett. 35 (1994) 941.
[67] K.A. Campbell, M.R. Lashley, J.K. Wyatt, M.H. Nantz, R. David Britt, J. Am. Chem. Soc. 123 (2001) 5710.
[68] A. Chellamani, N.M.I. Alhaji, S. Rajagopal, R. Sevvel, C. Srinivasan, Tetrahedron 51 (1995) 12677.
[69] A. Chellamani, N.M.I. Alhaji, Indian J. Chem. A 38 (1999) 888.
[70] E.G. Samsel, K. Srinivasan, J.K. Kochi, J. Am. Chem. Soc. 107 (1985) 7606.
[71] H. Jacobsen, L. Cavallo, Organometallics 25 (2006) 177.
[72] A.R. Katritzky, J.M. Lagowski, Chemistry of the Heterocyclic N-Oxides, Academic Press, New York, 1971.
[73] G. Caron, P.A. Carrupt, B. Testa, G. Ermondi, A. Gasco, Pharm. Res. 13 (1996) 1186.
[74] D. Feichtinger, D.A. Plattner, Chem. Eur. J. 7 (2001) 591.
[75] J.E. Bahraoui, O. Wiest, D. Feichtinger, D.A. Plattner, Angew. Chem., Int. Ed. 40 (2001) 2073.
[76] G. Fatima Jeyanthi, K.P. Elango, Int. J. Chem. Kinet. 35 (2003) 154.
[77] H.M. Neu, T. Yang, R.A. Baglia, T.H. Yosca, M.T. Green, M.G. Quesne, S.P. de Visser, D.P. Goldberg, J. Am. Chem. Soc. 136 (2014) 13845.
[78] R.T. Sabapathy Mohan, M. Gopalakrishnan, M. Sekar, Tetrahedron 37 (1994) 10933.
[79] R.T. Sabapathy Mohan, M. Gopalakrishnan, M. Sekar, Tetrahedron 37 (1994) 10945.
[80] D.G. Lee, K.C. Brown, J. Am. Chem. Soc. 104 (1982) 5076.
[81] G. Licini, M. Bonchio, G. Modena, W.A. Nugent, Pure Appl. Chem. 71 (1999) 463.
[82] M.J. Zdilla, J.L. Dexheimer, M.M. Abu-Omar, J. Am. Chem. Soc. 129 (2007) 11505.
[83] O. Exner, in: N.B. Chapman, J. Shorter (Eds.), Advances in linear free energy relationships, Plenum Press, New York, 1972, p. 12.
[84] D.G. Lee, L.N. Congson, Can. J. Chem. 68 (1990) 1774.
[85] A. Thirumoorthi, D.S. Bhuvaneshwari, K.P. Elango, Int. J. Chem. Kinet. 42 (2010) 159.
[86] J. Nakazawa, H. Ogiwara, Y. Kashiwazaki, A. Ishii, N. Imamura, Y. Samejima, S. Hikichi, Inorg. Chem. 50 (2011) 9933.
[87] R. Sevvel, S. Rajagopal, C. Srinivasan, N.M.I. Alhaji, A. Chellamani, J. Org. Chem. 65 (2000) 3334.
[88] S.K. Crossno, L.H. Kalbus, G.E. Kalbus, J. Chem. Ed. 73 (1996) 175.
[89] O. Exner, J. Chem. Soc. Perkin Trans. 2 (1993) 973.